MotifGPL: Motif-Enhanced Graph Prototype Learning for Deciphering Urban Social Segregation

Tengfei He, Xiao Zhou*

Gaoling School of Artificial Intelligence, Renmin University of China
hetengfei121@ruc.edu.cn, xiaozhou@ruc.edu.cn

Abstract

Social segregation in cities, spanning racial, residential, and income dimensions, is becoming increasingly diverse and severe. As urban spaces and social dynamics grow more complex, residents experience varying levels of segregation, which, if left unaddressed, could exacerbate crime rates, fuel social tensions, and lead to other societal challenges. Effectively addressing these issues requires a comprehensive analysis of the underlying structures of urban spaces and resident interactions. While previous studies have primarily focused on surface-level indicators of segregation, they often fail to explore the complexity of urban structure and mobility dynamics, leaving gaps in understanding modern segregation patterns. To fill this gap, we propose the **Motif-Enhanced Graph Prototype Learning (MotifGPL)** framework, offering a novel approach to studying urban segregation. The framework consists of three key modules: *prototype-based graph structure extraction*, *motif distribution discovery*, and *urban graph reconstruction*. Specifically, we use prototype-based learning to extract key urban graph prototypes from both spatial and origin-destination graphs, incorporating attributes such as points of interest, street images, and flow indices. The motif distribution discovery module enhances interpretability by matching each prototype to similar motifs, which represent simplified graph structures that reflect local patterns. These motifs are then used to guide the reconstruction of urban graphs, enabling a more detailed exploration of spatial structures and mobility patterns. By identifying critical motifs influencing urban segregation, MotifGPL offers insights to guide the design of urban environments that can help reduce segregation. Experimental results demonstrate that MotifGPL effectively uncovers these key motifs and provides actionable insights for mitigating segregation.

Code — https://github.com/tengfeihe/MotifGPL

Introduction

Segregation refers to the differentiation of individuals from different population groups in either spatial or social dimensions, a phenomenon influenced by complex social contexts of environments (Oka and Wong 2019). Residential segregation is a common phenomenon in global urban development. Previous studies have suggested a strong connection

---

*corresponding author

between residential segregation and issues such as disparities in educational distribution (Quillian 2014; Owens and Rich 2023), unequal employment opportunities (Bursell and Bygren 2023), and the uneven allocation of public infrastructure, including healthcare services (White, Haas, and Williams 2012; Seewaldt and Winn 2023). These imbalances caused by residential segregation can exacerbate tensions between residents, potentially leading to collective conflicts and regional unrest.

As urbanization advances, the growing complexity and diversity of urban areas are expanding social segregation beyond residential areas, leading to new forms of separation in social and economic realms (Lens and Monkkonen 2016). Currently, income segregation is emerging as a significant issue in metropolises, restricting interactions among different groups. As Florida (2017) points out, rising income segregation strengthens social boundaries, reducing interactions between social classes and deepening societal divides. These different forms of segregation reinforce each other, creating multi-layered segregation within cities. Without effective policy interventions, these patterns of segregation may reinforce themselves, preventing sustainable development. Therefore, a better understanding of social segregation and the implementation of effective solutions are crucial for promoting urban development.

To explore and understand urban social segregation, sociologists have traditionally relied on static socioeconomic data to develop comprehensive indicators reflecting segregation levels. Massey and Denton (1988) initially categorized urban segregation into five primary dimensions, which Brown and Chung (2006) later distilled into two main dimensions: concentration-evenness and clustering-exposure. Building on this, Kwan (2013) introduced an additional accessibility indicator, utilizing these three metrics to assess segregation levels. The advent of digitalization in urban environments has enriched the datasets available for segregation studies, offering a more dynamic perspective. Researchers have begun employing mobility data to track individual movement patterns within cities and to examine spatial accessibility (Chen et al. 2018). Furthermore, Moro et al. (2021) demonstrated that severe income segregation can persist even in geographically proximate areas, highlighting the necessity of accounting for both urban spatial configurations and mobility patterns in segregation assess-

ments.

Alongside the expansion of data types, innovative methodologies have been incorporated into segregation research. Sousa and Nicosia (2022) utilized urban network structures to model racial segregation and employed graph random walks to explore the spatial diversity of racial distributions. Similarly, Zhang et al. (2021) leveraged mobility data and community detection algorithms to investigate income-economic segregation, analyzing movement patterns across different socioeconomic strata. These advancements not only broaden the scope of data used but also introduce new analytical techniques for more effectively dissecting complex social phenomena.

While extensive research has focused on quantifying social segregation using established metrics, these studies often lack depth in their interpretative analyses. Existing research frequently limits the use of mobility and urban spatial data to descriptive statistics, without exploring their potential to reveal deeper insights into segregation dynamics. Emerging technologies like deep learning are rarely applied to the study of social segregation, primarily due to a traditional reliance on established statistical methods. This underutilization of advanced technologies restricts the depth of analysis, preventing a more thorough exploration of the complex causes and patterns that characterize urban social segregation. Embracing these technologies could enhance the interpretability of segregation studies, offering deeper insights into the underlying mechanisms and facilitating a more comprehensive understanding of both the immediate and systemic factors driving segregation. This approach not only enriches the analytical landscape but also strengthens the potential for developing more effective interventions.

To address existing challenges, we introduce a framework named **Motif**-Enhanced **G**raph **P**rototype **L**earning (**MotifGPL**), incorporating interpretable deep learning methods to analyze social segregation through urban graph structures and mobility patterns. MotifGPL consists of three main components: prototype-based graph structure extraction, motif distribution discovery, and urban graph structure reconstruction. Our research leverages multimodal social data, which include socioeconomic indicators, population flow indices, **points of interest** (**POIs**), street view images, urban spatial graph, and **origin-destination** (**OD**) graph among other diverse information sources. Specifically, we first map this data onto nodes and edges of the urban graph to accurately reflect urban complexity. We then employ a prototype network graph feature extractor to encode the urban graph and learn prototype vectors that represent various socioeconomic states, capturing the essential features of social segregation. Through motif distribution discovery techniques, we delve into the fundamental structural patterns of the urban graph, essential for deciphering the micro-mechanisms of social segregation.

We focus on the segregation index (Moro et al. 2021) as a supervisory signal for our model's learning, enhancing interpretability and providing new insights into the dynamics of segregation. This metric aids in identifying and analyzing local structures within the urban graph and helps quantify the extent and patterns of social segregation. Our experimental results demonstrate that MotifGPL effectively identifies the key factors influencing urban social segregation at the motif pattern level, offering robust support for strategies aimed at reducing this issue. Our contributions are summarized as follows:

- We propose a framework that analyzes social segregation by focusing on urban structures and mobility, effectively addressing the complexities of urban social segregation.

- Our model provides significant interpretability through motif distribution discovery, offering a deeper understanding of how urban structures contribute to social segregation and demonstrating a clear link between theoretical models and real-world urban dynamics.

- Our model offers actionable strategies for urban planning by utilizing motif analysis, which can effectively reduce segregation and foster urban sustainable development.

Related Work

Social Segregation Assessment The concept of segregation, originally derived from sociological studies on racial segregation in cities, has had a profound impact on urban economies. For instance, segregation in the United States led to considerable economic disparities, including a \$3 billion loss for Black residents in Chicago, alongside skewed public resource allocation (Wang et al. 2018). As urban dynamics have evolved, segregation now spans racial, residential, and income dimensions, intensifying as critical urban development challenges (Gottdiener, Hohle, and King 2019).

Addressing urban segregation requires robust quantification of the issue. Massey and Denton (1988) initially categorized social segregation into five indicators: evenness, exposure, concentration, centralization and clustering. Later, Brown and Chung (2006) simplified these to concentration and exposure for a more effective assessment. However, as urban functions and mobility patterns grow increasingly complex, these traditional indicators often fall short. Kwan (2013) introduced accessibility as an additional dimension, providing a more comprehensive framework to assess segregation from both spatial and individual perspectives.

Existing methods typically assign a degree indicator to each block to reflect one aspect of segregation. While these methods provide a straightforward reflection of segregation distribution, they fail to uncover the structural information related to social segregation within urban spatial structures and population mobility.

Graph Learning in Social Computing Modeling cities as graphs that incorporate edge information, rather than merely calculating statistical features of urban blocks, provides a richer representation of the city. Graph neural networks (Scarselli et al. 2008) are effective for embedding and predicting features in urban graph networks. Researchers (Huang et al. 2023b; Jin et al. 2023; Zou et al. 2024) use graph learning to analyze urban characteristics, dividing tasks into urban graph embedding (Li et al. 2024; Yan et al. 2024) and graph representation learning (Li et al. 2023; Jin et al. 2023; Khoshraftar and An 2024). These tasks facilitate aligning diverse data—from POIs (Huang et al.

2023b) to street view images (Yong and Zhou 2024) and mobility data (Huang et al. 2023a)—into a unified feature space, which is then used to derive node attributes for downstream applications such as crime rate prediction (Xu and Zhou 2024), real estate price forecasting (Brimos et al. 2023) and light pollution prediction(Zhang, Guo, and Zhou 2024).

Focusing on social segregation, He et al. (2020) utilized social graph data to analyze individual mobility patterns and observe residential segregation from a personal perspective. Yabe et al. (2023) examined the effects of the COVID-19 pandemic on income segregation in U.S. cities using mobile signaling and statistical data. Additionally, graph community detection algorithms (Zhang et al. 2021; Cavallari et al. 2017) have been applied to analyze urban income segregation, offering new insights for segregation studies.

Interpretability in Social Computing In the field of graph deep learning, there is a growing emphasis on the importance of model interpretability, particularly for addressing complex sociological issues such as social segregation. Understanding the reasoning behind model outputs is crucial for effectively tackling these societal challenges. Kakkad et al. (2023) categorizes interpretable graph models into post-hoc (Baldassarre and Azizpour 2019; Ying et al. 2019; Zhang et al. 2022a) and self-explainable (Zhang et al. 2022b; Seo, Kim, and Park 2024; Chen and Ying 2024) models. Post-hoc explanations analyze a trained model's weights to explain predictions, while self-explainable models integrate information or structural constraints during training to provide inherent explanations.

Incorporating deep learning into sociological studies enhances the uncovering of hidden information, thus improving our understanding of intricate social issues. Fan et al. (2023) introduced an interpretable framework that elucidates complex interactions among urban variables to address income inequality. Tang, Xia, and Huang (2023) added interpretability to spatiotemporal GNNs, enhancing predictions of traffic flow and urban space. Zhou et al. (2024) developed an interpretable model for simulating crowd movements, offering insights into urban dynamics. Similarly, Ding et al. (2024) employed motif discovery algorithms to provide a deeper understanding of the factors influencing tourist attractions.

Although these studies provide valuable tools for exploring urban issues, there is currently a lack of research that combines motif discovery with self-explainable graph learning frameworks to tackle urban problems.

Preliminaries

In this section, we introduce the urban graph structure, regional attribute data types, and the calculation of social segregation indices, outlining how these elements are integrated to effectively analyze urban social segregation.

Urban Graph Cities consist of distinct blocks, each with unique geographical locations, traffic patterns, and commercial structures, which together form the city's fundamental geographic structure. Within this space, the movement of residents and the exchange of information between blocks create an urban OD graph. Thus, a city is represented by a graph $\mathcal{G} = (\mathcal{G}_s, \mathcal{G}_o)$, where $\mathcal{G}_s = (\mathcal{V}, \mathcal{E}_s)$ is the geographic spatial graph and $\mathcal{G}_o = (\mathcal{V}, \mathcal{E}_o)$ denotes the residents' OD graph. Here, $\mathcal{V}$ represents the city blocks, $\mathcal{E}_s$ the set of geographic proximity edges, and $\mathcal{E}_o$ the flow edges depicting resident movements. The adjacency matrices $A_s = (a_{ij}^s \in \{0,1\}), \forall i,j \in [1, \| \mathcal{V} \|]$ and $A_o = (a_{ij}^o \in \{0,1\}), \forall i,j \in [1, \| \mathcal{V} \|]$ correspond to $\mathcal{G}_s$ and $\mathcal{G}_o$, respectively.

Region Attributes Regional attributes encompass both the geographical and social characteristics of city blocks. Street view data capture the geographical features of a block, the regional pedestrian flow index highlights its importance within the urban mobility framework, and POIs data reflect a block's role in the urban functional layout. Socioeconomic indicators represent the social characteristics of residents and measure the degree of social segregation. For each block $v_i \in \mathcal{V}$, we define X_i^{SV} as the street view data, X_i^{FL} as the pedestrian flow index, X_i^{POI} as the count of various POIs, and X_i^{SE} as the socioeconomic indicators. The metrics X^{SV}, X^{FL}, X^{POI}, and X^{SE} collectively represent these attributes for the entire block set $\mathcal{V}$.

Network Motifs Network motifs are recurrent local connection patterns in complex network structures, serving as fundamental components that encapsulate the network's architecture. In prototype learning, each prototype $\mathbf{p}_i$ in the matrix $\mathbf{P}$ is associated with a motif pattern distribution $\mathbf{m}_i$, derived from the local graph structure most similar to $\mathbf{p}_i$. This distribution $\mathbf{m}_i$ reflects the local structural information of the node subset $\mathcal{V}_i$ that closely resembles the prototype.

Social Segregation Index We collected aggregated socioeconomic indicators for each block, including average income levels, average education levels, and the average age of residents. Following Moro et al. (2021), we used the segregation index to calculate social segregation within each block, defined as follows:

$$S_i = \frac{c}{2(c-1)} \sum_k^c \left| \tau_{ci} - \frac{1}{c} \right|, \qquad (1)$$

where τ is the economic distribution (e.g., income, education, and age) and c is the dimension.

This segregation index quantifies differences in segregation levels across blocks and categorizes them into two classes based on quantiles to identify blocks with social segregation, providing a foundation for analyzing how urban networks influence segregation.

Problem Statement

Given an urban geographic spatial graph $\mathcal{G}_s = (\mathcal{V}, \mathcal{E}_s)$ and an OD graph $\mathcal{G}_o = (\mathcal{V}, \mathcal{E}_o)$ with their corresponding adjacency matrices A_s and A_o, and node attributes $X = (X^{SV} \| X^{FL} \| X^{POI})$, we aim to use the degree of social segregation $\mathbf{d}^{SEG}$, derived from socioeconomic indicators X^{SE}, as a supervisory signal to learn prototypes $\mathbf{P}$ related to urban social segregation and their corresponding motif distribution $\mathbf{M}$. The learning task is formalized as follows:

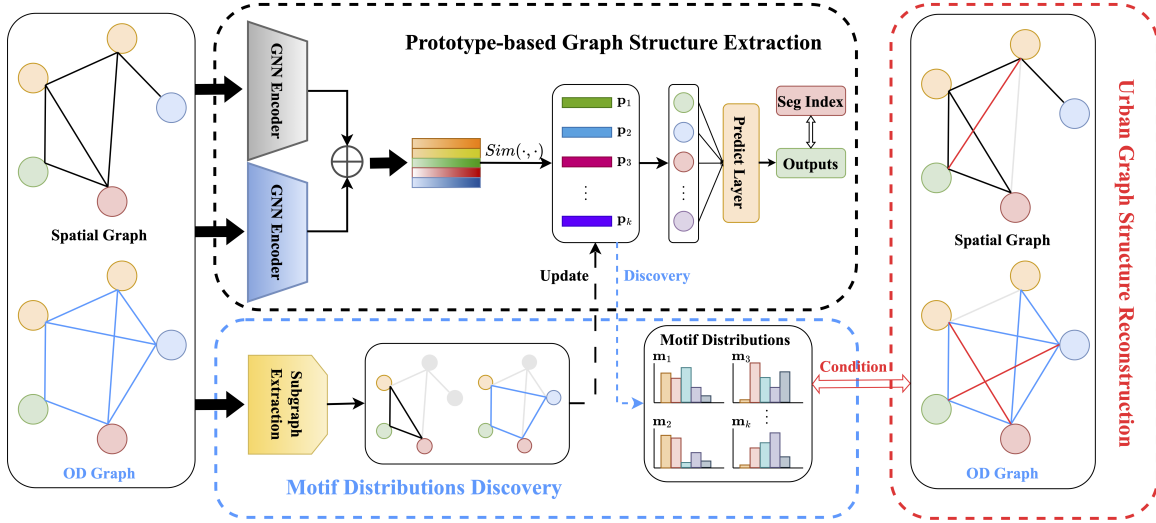$$F : \mathcal{D} \rightarrow M \in \mathrm{R}^{q \times d}, \qquad (2)$$

Figure 1: The framework of Motif-Enhanced Graph Prototype Learning (MotifGPL).

where $\mathcal{D} = \langle \mathcal{G}_s, \mathcal{G}_o, A_s, A_o, X \rangle$, q represents the number of prototypes, and d denotes the dimension of the motif distribution. F is a function that uses data from both graphs to compute motif distributions associated with the prototypes. Subsequently, we will utilize the motif distributions to guide the optimization of urban graph structures, aiming to reduce social segregation within cities.

Methodology

Framework Overview

Figure 1 illustrates our framework for identifying local structures associated with social segregation from spatial and OD graphs. The model comprises three main components: the **prototype-based graph structure extraction module**, the **motif distribution discovery module**, and the **urban graph structure reconstruction module**.

The prototype-based graph structure extraction module involves encoding multi-attribute and graph structure information, followed by prototype learning guided by social segregation degree indicators. The motif distribution discovery module then projects these prototypes onto the spatial and OD graphs to identify local node structures and extract motif distributions. Finally, the urban graph structure reconstruction module utilizes these motif distributions to optimize the urban spatial graph structure, with the goal of alleviating social segregation in cities.

Prototype-based Graph Structure Extraction

Graph Encoder The urban spatial graph $\mathcal{G}_s$ considers the connectivity of urban areas based on geographical proximity. Following Tobler's first law of geography, we use the spatial graph to simplify inter-regional connections within cities, focusing on links between neighboring areas within a specified threshold. Conversely, the OD graph $\mathcal{G}_o$ represents connections based on population mobility.

Our model employs two feature extractors to independently encode $\mathcal{G}_s$ and $\mathcal{G}_o$ using adjacency matrices A_s and A_o and node attributes X. We utilize Graph Neural Networks (GNNs) as encoders to integrate graph structural information through a multi-layer message passing mechanism. The message passing formula is defined as follows:

$$H_m^{(l+1)} = \sigma \left(\tilde{D}_m^{-\frac{1}{2}} \tilde{A}_m \tilde{D}_m^{-\frac{1}{2}} H_m^{(l)} W_m^{(l)} \right), \qquad (3)$$

where $m = \{s, o\}$ specifies encoders for $\mathcal{G}_s$ or $\mathcal{G}_o$. $\tilde{A}_m = A_m + I_N$ includes self-loops, $\tilde{D}_m$ is the degree matrix, $\tilde{W}_m^{(l)}$ is the layer-specific weight matrix, and σ typically refers to the ReLU activation function. $H^{(0)} = X$ represents the initial node attributes. To fully leverage the structural information from both graphs, we concatenate the outputs from each layer of the GNN encoders, resulting in a node latent space representation that blends features from both $\mathcal{G}_s$ and $\mathcal{G}_o$.

Following the encoding, the node attributes and graph structure are transformed into a latent space representation, denoted as $\mathbf{H}$. In the prototype learning layer, we maintain a fixed number (N_{proto}) of prototypes per class, capturing essential local structures. Similarity scores s_{ij} between each node's latent representation $\mathbf{h}_i$ and prototype $\mathbf{p}_j$ are calculated as follows:

$$s_{ij} = \log \left(\frac{\| \mathbf{h}_i - \mathbf{p}_j \|_2^2 + 1}{\| \mathbf{h}_i - \mathbf{p}_j \|_2^2 + \epsilon} \right), \qquad (4)$$

where ϵ is a small constant for numerical stability. The similarity scores inform a fully connected layer with softmax activation to classify nodes.

Motif Distribution Discovery

Prototype Projection Though prototype vectors are continuously optimized during training, they often lack intuitive interpretability. To address this, we developed a module that projects prototype vector $\mathbf{p}_i$ onto local subgraphs $\mathcal{G}_{sub}$ of

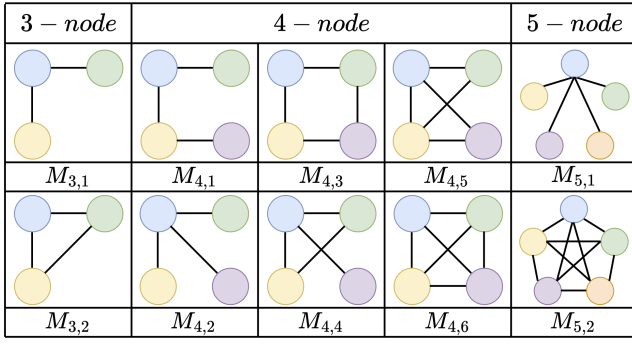| $3-node$	$4-node$			$5-node$
$M_{3,1}$	$M_{4,1}$	$M_{4,3}$	$M_{4,5}$	$M_{5,1}$
$M_{3,2}$	$M_{4,2}$	$M_{4,4}$	$M_{4,6}$	$M_{5,2}$

Figure 2: Network motifs employed in the study. The blue node represents the target node, while the other nodes represent its neighbors.

nodes from category k within the graph $\mathcal{G}$ during training. This projection enhances the interpretability of the prototype vectors by associating them with the local structures of specific node categories. For a given node i, with the representation l_i denoting its local structure, the projection of prototype vectors is facilitated by the following process:

$$\mathbf{p}_k = \arg\min_{l_i \in L_i} \| l_i - \mathbf{p}_k \|_2, \qquad (5)$$

$$L_i = \{f_{sub}(\mathcal{G}_{sub}^i); \ \mathcal{G}_{sub}^i \in \text{Sub}(\mathcal{G}^i) \ \forall i \ \text{s.t.} \ y_i = k\}. \quad (6)$$

To efficiently classify nodes in large-scale graphs, we developed a random-walk-based local structure extractor. For each node i, this extractor generates r random walk sequences, each of length t:

$$s_{j+1} = \text{Random}(\omega_j \mathcal{N}(s_j)), \qquad (7)$$

$$T^i \in \mathrm{R}^{r \times t}, \quad where \quad t_k^i = (s_0^k, s_1^k, \cdots, s_t^k), \quad (8)$$

where s_j denotes the currently selected node in the random walk, and ω_j represents the weight of the edge connecting to neighbors. T^i represents the local graph structure of node i. Subsequently, we use a RNN to encode this local structure into latent space, matching the prototype's dimension, resulting in the encoded structure $l_i = \text{RNNEncoder}(T^i)$.

Motifs Detection Each prototype is aligned with the local structure of a node within its category through prototypical projection, utilizing random walk sequences. These sequences are then reconstructed into a subgraph for each prototype, providing a subgraph representation. Building on this, we initiate motif discovery, where motifs are defined as statistically overrepresented substructures in networks (Milo et al. 2002). In a real network and N random networks, a subgraph qualifies as a motif if it meets the following conditions, with a probability threshold P_M:

$$p((f_{rand}(G_k) > f_{real}(G_k))) \le P_M, \qquad (9)$$

where $f_{real}(G_k)$ is the frequency of a motif in real network G_k, and $f_{rand}(G_k)$ is the average frequency in all random networks about G_k.

The main advantage of motifs is the ability to capture the core connectivity of a network with fewer nodes and edges,

maintaining a balance between complexity and interpretability. Too few nodes miss critical structural patterns, whereas too many reduce motif clarity. We focus on 3-node, 4-node, and selected 5-node motifs, as shown in Figure 2, to provide detailed insights into urban social segregation from a structural perspective. For each subgraph G_k associated with a prototype $\mathbf{p}_k$, we count the frequency of the motif, forming the motif distribution m_k for the current prototype.

Urban Graph Structure Reconstruction

The motif distribution derived from prototype vectors enables a thorough analysis of the spatial and mobility mechanisms influencing social segregation in cities. We use this distribution to guide the reconstruction of the urban graph. After establishing the motif distribution $\mathbf{M}$, we assign the corresponding motif distribution m_i to each node, based on its local network structure $\mathcal{G}_i^{sub}$. With a reconstruction threshold α, we incrementally adjust the adjacency matrix A for nodes in a specific category. The steps are as follows:

$$m_i^G \leftarrow \arg\max_{m_k \in \mathbf{M}} \ \text{Sim}(\text{Motif}(\mathcal{G}_i^{sub}), m_k), \qquad (10)$$

$$A[i] = (1 - \alpha\text{KL})A[i] + (\alpha\text{KL})A[tar], \qquad (11)$$

$$\text{KL} = KL(m_i^G, m_{tar}^G), \qquad (12)$$

$$A_{ij}^{\text{new}} = \begin{cases} 1 & \text{if } A_{ij} > \beta \\ 0 & \text{if } A_{ij} \le \beta, \end{cases} \qquad (13)$$

where $\mathcal{G}_i^{sub}$ denotes the subgraph of $\mathcal{G}$ with node i and $A[i]$ denotes the i-th row of adjacency matrix. $KL(\cdot, \cdot)$ signifies the KL divergence, α represents the reconstruction weight factor, and β stands for the edge creation threshold.

Optimization

During training, our objective is to understand the network structure underlying urban social segregation, using the social segregation index $\mathbf{d}^{SEG}$ as the ground truth. We enhance model's accuracy in predicting social segregation levels by minimizing the cross-entropy loss function $\mathcal{L}_{CrsEtp}$. In the prototype learning layer, we improve prototype interpretability by imposing constraints that refine their ability to capture key local structures. Following Zhang et al. (2022b), we incorporate a cluster loss $\mathcal{L}_{Clst}$, encouraging nodes to align more closely with their respective prototype vectors, and a separation loss $\mathcal{L}_{Sprt}$, which distances nodes from non-category prototypes. Additionally, in the motif detection module, we apply an encoding loss $\mathcal{L}_{Enc}$ to ensure the local subgraph encoder learns the optimal representation from subgraphs to prototype vectors. In summary, the loss functions we aim to optimize are as follows:

$$\mathcal{L}_{CrsEtp} = \frac{1}{n} \sum_{i=1}^{N} \sum_{c=1}^{C} y_i^c \log(g_{\mathbf{p}}(h_i^c)), \qquad (14)$$

$$\mathcal{L}_{Clst} = \frac{1}{n} \sum_{i=1}^{N} \min_{j:\mathbf{p}_j \in \mathbf{P}_{y_j}} \| g_{\mathbf{p}}(h_i) - \mathbf{p}_j \|_2^2, \qquad (15)$$

$$\mathcal{L}_{Sprt} = -\frac{1}{n} \sum_{i=1}^{N} \min_{j:\mathbf{p}_j \notin \mathbf{P}_{y_j}} \| g_{\mathbf{p}}(h_i) - \mathbf{p}_j \|_2^2, \qquad (16)$$

$$\mathcal{L}_{Enc} = \frac{1}{p} \sum_{k=1}^{p} \min_{i:\mathcal{G}_{sub}^i \in \mathcal{G}_{sub}(y_i=k)} \| f_{sub}(\mathcal{G}_{sub}^i) - \mathbf{p}_k \|_2^2, \tag{17}$$

where N denotes the number of block nodes, C represents the number of segregation levels, y_i^c is the true label of node i, and $g_{\mathbf{p}}(\cdot)$ is the function of prototype layer. $\mathbf{P}_{y_j}$ represents the set of prototype vectors belonging to the same class as y_i, p denotes the number of prototypes, f_{sub} is the function of the subgraph encoder, and $\mathcal{G}_{sub}^i$ is the subgraph centered at node i. Combining these loss functions, the overall objective function is as follows:

$$\mathcal{L} = \mathcal{L}_{CrsEtp} + \lambda_1 \mathcal{L}_{Clst} + \lambda_2 \mathcal{L}_{Sprt} + \lambda_3 \mathcal{L}_{Enc}. \tag{18}$$

Experiments

Datasets Beijing has evolved unique residential spatial distribution and mobility patterns during urban expansion, making it an ideal city for studying urban social segregation. We selected Beijing as the study city and divided it into 2104 blocks based on geographical divisions. To focus on social segregation in the urban core, we sampled 842 blocks within a 10-kilometer radius of the city center. The dataset includes a spatial graph $\mathcal{G}_s(\| \mathcal{V} \| = 842, \| \mathcal{E} \| = 6132)$ and an OD graph $\mathcal{G}_o(\| \mathcal{V} \| = 842, \| \mathcal{E} \| = 36334)$. Each block contains data on 21 categories of POIs, hourly pedestrian flow indices, and 20 street view images for both summer and winter, obtained through uniform sampling within the block boundaries.

Baselines In the experiments, we select GNN variants such as GCN (Kipf and Welling 2016), GAT (Veličković et al. 2017), and GIN (Xu et al. 2018), along with interpretable models like ProtGNN (Zhang et al. 2022b) and PGIB (Seo, Kim, and Park 2024). To better evaluate the improvements brought by graph prototype learning to GNN models, we also include GAT and GIN models augmented with the prototype framework. Through comparative analyses, we assess the effectiveness of our model in accurately predicting social segregation levels.

Experimental Settings In the social segregation levels prediction task, we split the data into training, validation, and test sets with proportions of 0.6, 0.2, and 0.2, respectively. The social segregation index serves as the training label for the prototype network. A pre-trained ResNet50 (He et al. 2016) is used to encode street view images, which are then combined with POIs and flow indices to generate 256-dimensional node attributes. These node attributes are subsequently mapped into a 128-dimensional latent space using a GNN module. The learning parameters are set as follows: a learning rate of 0.001, a maximum of 3000 epochs, and a prototype projection interval of 50 epochs. The hyperparameters for the objective function are $\lambda_1 = 0.4, \lambda_2 = 0.2, \lambda_3 = 2$. A crucial hyperparameter is the number of prototype vectors per class (N_{proto}), which is set to 5 based on preliminary experiments. These experiments show that five prototypes optimize both efficiency and interpretability. Using more prototypes increases training time, while fewer prototypes reduces motif discovery. Additionally, to ensure robustness, each experiment is repeated five times.

	Segregation Index	
	Accuracy (↑)	*F1−score* (↑)
GCN	0.7872±0.0002	0.7854±0.0002
GAT	0.7692±0.0006	0.7686±0.0006
GIN	0.7512±0.0008	0.7508±0.0008
ProtGNN	0.7348±0.0014	0.7384±0.0016
PGIB	0.7502±0.0010	0.7626±0.0008
GAT+Prototype	0.7896±0.0001	0.7884±0.0001
GIN+Prototype	0.7644±0.0006	0.7640±0.0005
MotifGPL	**0.7990±0.0005**	**0.7976±0.0006**

Table 1: Evaluation of social segregation classification.
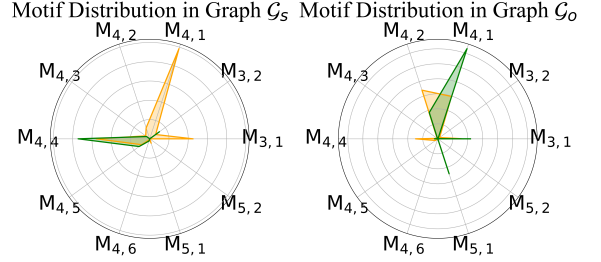

Figure 3: Motif distribution of prototypes in $\mathcal{G}_s$ and $\mathcal{G}_o$.

Experimental Results

Social Segregation Levels Classification Task We assess the model's performance in predicting segregation levels. The results in Table 1 show that: 1) Compared to GCN, GAT, and GIN models, MotifGPL achieves the best performance in the prediction task. Furthermore, it offers a significant advantage in interpretability. While GNN models like GCN, GAT, and GIN are opaque box models without interpretability, which limits the investigation of social segregation, our graph prototype learning framework captures valuable information and improves interpretability through low-dimensional prototype vectors. 2) Compared to GNN interpretability methods like ProtGNN and PGIB, which are optimized for graph classification and underperform on node classification, our model achieves higher accuracy while maintaining interpretability. The prototype vectors in our model capture key factors related to social segregation, improve performance on node-level tasks, and support effective motif pattern discovery.

Motif Distribution Discovery Next, we employ graph isomorphism algorithms to identify motif patterns of trained prototype. Figure 3 shows the motif distribution corresponding to the prototypes of Graph $\mathcal{G}_s$ and $\mathcal{G}_o$, where green represents motifs of blocks with high segregation and orange indicates motifs of blocks with low segregation. In the spatial graph, motifs in high-segregation blocks are primarily found in $M_{4,4}$ and $M_{3,2}$. These circular motifs indicate that these blocks exhibit spatial clustering, forming enclosed community structures. In contrast, motifs in low-segregation blocks are concentrated in $M_{4,1}$, $M_{4,4}$, and $M_{3,1}$, with chain-like motifs suggesting a linear spatial distribution that enhances

	α	β	AEP	REP	UEP	Moran's I($\downarrow$)
$\mathcal{G}_s$	original		0.00	0.00	100.00	0.4159
	0.8	0.3	1.40	0.24	99.76	0.4043
	0.8	0.2	5.81	0.00	100.00	0.3751
	0.8	0.1	15.05	0.00	100.00	0.3169
$\mathcal{G}_o$	original		0.00	0.00	100.00	0.2410
	0.8	0.3	1.89	0.32	0.9968	0.2341
	0.8	0.2	8.14	0.00	100.00	0.2118
	0.8	0.1	19.92	0.00	100.00	0.1805

Table 2: Results of urban graph reconstruction. AEP denotes added edge percentage, REP denotes removed edge percentage, and UEP denotes unchanged edge percentage.
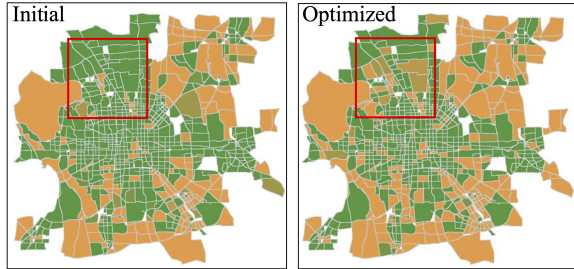

Figure 4: Comparison of reconstruction outcomes across block segregation levels (orange indicates low segregation, green indicates high segregation).

	Segregation Index	
	$Accuracy$ ($\uparrow$)	$F1-score$ ($\uparrow$)
MotifGPL	**0.7990±0.0005**	**0.7976±0.0006**
w/o $\mathcal{G}_o$	0.7776±0.0005	0.7758±0.0005
w/o $\mathcal{G}_s$	0.7212±0.0002	0.7210±0.0002
w/o X^{SV}	0.7834±0.0008	0.7814±0.0009
w/o X^{FL}	0.7752±0.0005	0.7734±0.0006
w/o X^{POI}	0.7560±0.0003	0.7534±0.0004

Table 3: Results of ablation study for MotifGPL.

which is unsuitable for dynamic network reconstruction. Global Moran's I ranges from -1 to 1, where a larger absolute value indicates higher spatial segregation. Table 2 presents the results of the urban graph structure reconstruction experiments. Here, α and β represent the reconstruction weight and edge generation threshold, respectively. The results indicate that using motif distribution to guide spatial or OD graph reconstruction reduces social segregation. At a low reconstruction level ($\alpha = 0.8, \beta = 0.3$), only minor changes ($<2.5\%$) to the existing urban structure are required to decrease social segregation. Figure 4 shows the changes in segregation levels in Beijing after urban graph reconstruction. Highlighted areas indicate that reconstruction can partially reduce social segregation. In practice, enhancing connectivity between blocks by improving infrastructure or adding new transportation routes is a feasible approach for urban graph structure reconstruction. Experiments show that motif patterns provide novel insights for guiding reconstruction.

Ablation Study We conduct ablation experiments on the classification task, focusing on graph structures and node attributes. As shown in Table 3, the results indicate that the absence of either the spatial graph or the OD graph leads to a decrease in performance, suggesting that the local structures of these two graphs are crucial for analyzing urban social segregation from the perspective of motif patterns. Similarly, the absence of any node attribute leads to reduced performance, indicating that the selected urban attribute data reflect various aspects of segregation.

Conclusion

This paper presents a framework called Motif-Enhanced Graph Prototype Learning (MotifGPL), which integrates motif discovery with graph prototype learning to uncover insights related to social segregation within urban spatial structures and population movement patterns. We explore motif patterns associated with social segregation, providing a new perspective for addressing segregation issues in urban environments. Our experimental results demonstrate that the motif patterns identified by the model have strong interpretability in real-world scenarios. This not only provides a novel methodological approach for investigating urban segregation but also offers substantial support for urban planning and development practices.

interaction with the urban environment. In the OD graph, the motif distribution of blocks with varying segregation levels is primarily concentrated in chain-like ($M_{4,1}$ and $M_{3,1}$) and star-like ($M_{4,2}$ and $M_{5,1}$) patterns. Comparing the number of motifs in $M_{4,1}$, high-segregation blocks contain significantly more chain-like motifs than low-segregation blocks, indicating that residents in high-segregation blocks endure longer commutes. Additionally, star-like motifs in high-segregation blocks are more complex than those in low-segregation blocks, suggesting that residents in segregated blocks often travel to centralized blocks for daily activities, reflecting a clear separation between living and working spaces. Based on these findings, urban planners should consider shifting from traditional clustered housing to a linear distribution strategy when selecting sites for new affordable housing developments to mitigate segregation among residents. Additionally, improving amenities around high-segregation blocks will help residents more easily meet their daily living and working needs.

Urban Graph Reconstruction Using the discovered motif distribution to guide the reconstruction of urban graph structures can facilitate minor modifications to the existing urban framework, ultimately reducing overall social segregation in the city. According to Garreton, Basauri, and Valenzuela (2020), we utilize Global Moran's I to measure the overall degree of social segregation across Beijing, as it captures spatial autocorrelation and reflects dynamic changes in segregation patterns, unlike the static segregation index,

Acknowledgments

References

Baldassarre, F.; and Azizpour, H. 2019. Explainability techniques for graph convolutional networks. *arXiv preprint arXiv:1905.13686*.

Brimos, P.; Karamanou, A.; Kalampokis, E.; Mamalis, M. E.; and Tarabanis, K. 2023. Explainable Graph Neural Networks on Linked Statistical Data for Predicting Scottish House Prices. In *Proceedings of the 27th Pan-Hellenic Conference on Progress in Computing and Informatics*, 36–41.

Brown, L. A.; and Chung, S.-Y. 2006. Spatial segregation, segregation indices and the geographical perspective. *Population, space and place*, 12(2): 125–143.

Bursell, M.; and Bygren, M. 2023. The making of ethnic segregation in the labor market: Evidence from a field experiment. Technical report, Working Paper.

Cavallari, S.; Zheng, V. W.; Cai, H.; Chang, K. C.-C.; and Cambria, E. 2017. Learning community embedding with community detection and node embedding on graphs. In *Proceedings of the 2017 ACM on Conference on Information and Knowledge Management*, 377–386.

Chen, B. Y.; Wang, Y.; Wang, D.; Li, Q.; Lam, W. H.; and Shaw, S.-L. 2018. Understanding the impacts of human mobility on accessibility using massive mobile phone tracking data. *Annals of the American Association of Geographers*, 108(4): 1115–1133.

Chen, J.; and Ying, R. 2024. Tempme: Towards the explainability of temporal graph neural networks via motif discovery. *Advances in Neural Information Processing Systems*, 36.

Ding, D.; Zheng, Y.; Zhang, Y.; and Liu, Y. 2024. Understanding attractions' connection patterns based on intra-destination tourist mobility: A network motif approach. *Humanities and Social Sciences Communications*, 11(1): 1–12.

Fan, C.; Xu, J.; Natarajan, B. Y.; and Mostafavi, A. 2023. Interpretable machine learning learns complex interactions of urban features to understand socio-economic inequality. *Computer-Aided Civil and Infrastructure Engineering*, 38(14): 2013–2029.

Florida, R. 2017. *The new urban crisis: How our cities are increasing inequality, deepening segregation, and failing the middle class-and what we can do about it*. Hachette UK.

Garreton, M.; Basauri, A.; and Valenzuela, L. 2020. Exploring the correlation between city size and residential segregation: comparing Chilean cities with spatially unbiased indexes. *Environment and urbanization*, 32(2): 569–588.

Gottdiener, M.; Hohle, R.; and King, C. 2019. *The new urban sociology*. Routledge.

He, K.; Zhang, X.; Ren, S.; and Sun, J. 2016. Deep residual learning for image recognition. In *Proceedings of the IEEE conference on computer vision and pattern recognition*, 770–778.

He, T.; Bao, J.; Li, R.; Ruan, S.; Li, Y.; Song, L.; He, H.; and Zheng, Y. 2020. What is the human mobility in a new city: Transfer mobility knowledge across cities. In *Proceedings of The Web Conference 2020*, 1355–1365.

Huang, L.; Xia, F.; Chen, H.; Hu, B.; Zhou, X.; Li, C.; Jin, Y.; and Xu, Y. 2023a. Reconstructing human activities via coupling mobile phone data with location-based social networks. *Travel behaviour and society*, 33: 100606.

Huang, W.; Zhang, D.; Mai, G.; Guo, X.; and Cui, L. 2023b. Learning urban region representations with POIs and hierarchical graph infomax. *ISPRS Journal of Photogrammetry and Remote Sensing*, 196: 134–145.

Jin, G.; Liang, Y.; Fang, Y.; Shao, Z.; Huang, J.; Zhang, J.; and Zheng, Y. 2023. Spatio-temporal graph neural networks for predictive learning in urban computing: A survey. *IEEE Transactions on Knowledge and Data Engineering*.

Kakkad, J.; Jannu, J.; Sharma, K.; Aggarwal, C.; and Medya, S. 2023. A survey on explainability of graph neural networks. *arXiv preprint arXiv:2306.01958*.

Khoshraftar, S.; and An, A. 2024. A survey on graph representation learning methods. *ACM Transactions on Intelligent Systems and Technology*, 15(1): 1–55.

Kipf, T. N.; and Welling, M. 2016. Semi-supervised classification with graph convolutional networks. *arXiv preprint arXiv:1609.02907*.

Kwan, M.-P. 2013. Beyond space (as we knew it): Toward temporally integrated geographies of segregation, health, and accessibility: Space–time integration in geography and GIScience. *Annals of the Association of American Geographers*, 103(5): 1078–1086.

Lens, M. C.; and Monkkonen, P. 2016. Do strict land use regulations make metropolitan areas more segregated by income? *Journal of the American Planning Association*, 82(1): 6–21.

Li, Y.; Huang, W.; Cong, G.; Wang, H.; and Wang, Z. 2023. Urban region representation learning with openstreetmap building footprints. In *Proceedings of the 29th ACM SIGKDD Conference on Knowledge Discovery and Data Mining*, 1363–1373.

Li, Z.; Huang, W.; Zhao, K.; Yang, M.; Gong, Y.; and Chen, M. 2024. Urban Region Embedding via Multi-View Contrastive Prediction. In *Proceedings of the AAAI Conference on Artificial Intelligence*, volume 38, 8724–8732.

Massey, D. S.; and Denton, N. A. 1988. The dimensions of residential segregation. *Social forces*, 67(2): 281–315.

Milo, R.; Shen-Orr, S.; Itzkovitz, S.; Kashtan, N.; Chklovskii, D.; and Alon, U. 2002. Network motifs: simple building blocks of complex networks. *Science*, 298(5594): 824–827.

Moro, E.; Calacci, D.; Dong, X.; and Pentland, A. 2021. Mobility patterns are associated with experienced income segregation in large US cities. *Nature communications*, 12(1): 4633.

Oka, M.; and Wong, D. W. 2019. Segregation: a multi-contextual and multi-faceted phenomenon in stratified societies. In *Handbook of urban geography*, 255–280. Edward Elgar Publishing.

Owens, A.; and Rich, P. 2023. Little boxes all the same? Racial-ethnic segregation and educational inequality across the urban-suburban divide. *RSF: The Russell Sage Foundation Journal of the Social Sciences*, 9(2): 26–54.

Quillian, L. 2014. Does segregation create winners and losers? Residential segregation and inequality in educational attainment. *Social Problems*, 61(3): 402–426.

Scarselli, F.; Gori, M.; Tsoi, A. C.; Hagenbuchner, M.; and Monfardini, G. 2008. The graph neural network model. *IEEE transactions on neural networks*, 20(1): 61–80.

Seewaldt, V. L.; and Winn, R. A. 2023. Residential racial and economic segregation and cancer mortality in the US—speaking out on inequality and injustice. *JAMA oncology*, 9(1): 126–127.

Seo, S.; Kim, S.; and Park, C. 2024. Interpretable prototype-based graph information bottleneck. *Advances in Neural Information Processing Systems*, 36.

Sousa, S.; and Nicosia, V. 2022. Quantifying ethnic segregation in cities through random walks. *Nature Communications*, 13(1): 5809.

Tang, J.; Xia, L.; and Huang, C. 2023. Explainable Spatio-Temporal Graph Neural Networks. In *Proceedings of the 32nd ACM International Conference on Information and Knowledge Management*, 2432–2441.

Veličković, P.; Cucurull, G.; Casanova, A.; Romero, A.; Lio, P.; and Bengio, Y. 2017. Graph attention networks. *arXiv preprint arXiv:1710.10903*.

Wang, Q.; Phillips, N. E.; Small, M. L.; and Sampson, R. J. 2018. Urban mobility and neighborhood isolation in America's 50 largest cities. *Proceedings of the National Academy of Sciences*, 115(30): 7735–7740.

White, K.; Haas, J. S.; and Williams, D. R. 2012. Elucidating the role of place in health care disparities: the example of racial/ethnic residential segregation. *Health services research*, 47(3pt2): 1278–1299.

Xu, K.; Hu, W.; Leskovec, J.; and Jegelka, S. 2018. How powerful are graph neural networks? *arXiv preprint arXiv:1810.00826*.

Xu, Z.; and Zhou, X. 2024. CGAP: Urban Region Representation Learning with Coarsened Graph Attention Pooling. *arXiv preprint arXiv:2407.02074*.

Yabe, T.; Bueno, B. G. B.; Dong, X.; Pentland, A.; and Moro, E. 2023. Behavioral changes during the COVID-19 pandemic decreased income diversity of urban encounters. *Nature communications*, 14(1): 2310.

Yan, Y.; Wen, H.; Zhong, S.; Chen, W.; Chen, H.; Wen, Q.; Zimmermann, R.; and Liang, Y. 2024. Urbanclip: Learning text-enhanced urban region profiling with contrastive language-image pretraining from the web. In *Proceedings of the ACM on Web Conference 2024*, 4006–4017.

Ying, Z.; Bourgeois, D.; You, J.; Zitnik, M.; and Leskovec, J. 2019. Gnnexplainer: Generating explanations for graph neural networks. *Advances in neural information processing systems*, 32.

Yong, X.; and Zhou, X. 2024. MuseCL: Predicting Urban Socioeconomic Indicators via Multi-Semantic Contrastive Learning. *arXiv preprint arXiv:2407.09523*.

Zhang, S.; Liu, Y.; Shah, N.; and Sun, Y. 2022a. Gstarx: Explaining graph neural networks with structure-aware cooperative games. *Advances in Neural Information Processing Systems*, 35: 19810–19823.

Zhang, T.; Duan, X.; Wong, D. W.; and Lu, Y. 2021. Discovering income-economic segregation patterns: A residential-mobility embedding approach. *Computers, Environment and Urban Systems*, 90: 101709.

Zhang, Y.; Guo, K.; and Zhou, X. 2024. Causally Aware Generative Adversarial Networks for Light Pollution Control. In *Proceedings of the AAAI Conference on Artificial Intelligence*, volume 38, 22529–22537.

Zhang, Z.; Liu, Q.; Wang, H.; Lu, C.; and Lee, C. 2022b. Protgnn: Towards self-explaining graph neural networks. In *Proceedings of the AAAI Conference on Artificial Intelligence*, volume 36, 9127–9135.

Zhou, Q.; Lu, X.; Gu, J.; Zheng, Z.; Jin, B.; and Zhou, J. 2024. Explainable Origin-Destination Crowd Flow Interpolation via Variational Multi-Modal Recurrent Graph Auto-Encoder. In *Proceedings of the AAAI Conference on Artificial Intelligence*, volume 38, 9422–9430.

Zou, X.; Yan, Y.; Hao, X.; Hu, Y.; Wen, H.; Liu, E.; Zhang, J.; Li, Y.; Li, T.; Zheng, Y.; et al. 2024. Deep learning for cross-domain data fusion in urban computing: Taxonomy, advances, and outlook. *arXiv preprint arXiv:2402.19348*.